paper reference: 2C.74

Fatigue life prediction of Natural Rubber components under uniaxial and multiaxial loading

N. Saintier, G. Cailletaud, R. Piques

Centre des matériaux P.M. FOURT,
Ecole Nationale Supérieure des Mines de Paris.
UMR CNRS 866, Evry cedex 91003, France,
E–mail: nsaintie@mat.ensmp.fr

1 Abstract

Experimental and numerical aspects of fatigue crack initiation are investigated. Using SEM observations, it is possible to observe fatigue cracks at initiation. Cracks were found to initiate on rigid particles, where cavitation and dewettering can be observed. A fatigue crack initiation criterion is proposed. Based on a critical plane aproach, the model is designed to consider the reinforcing effect of positive loading ratio in crystallizing elastomers. Validation of the model is achieved by comparing the predictions and the experimental data of several loading conditions.

2 Introduction

Modern technology has developed many applications in wich fatigue damage must be assessed to assure reliable and safe performance of structural components. Fatigue behavior of metallic materials has been explored for years and numerous fatigue criterion are proposed to predict fatigue failure under multiaxial loading. The major role played by elastomers in antivibration technologies, has made of importance to take into account fatigue of elastomeric materials in ingineering design. In practice, such components are subjected to multiaxial loading at temperatures close to room temperature. In this paper, multiaxial fatigue life of a natural rubber (N.R.) is investigated.
Cut growth studies on Natural Rubber (N.R.) have been reported by many authors [1] [2] . Most of these studies are dealing with precracked specimens and correlate the crack growth rate with the tearing energy. Fewer studies concern fatigue crack initiation in unprecracked specimens even though it is the case in practice. Indeed, subjecting a specimen to repeated extensions will produce small cracks which, by growing, conduct to the final failure of the specimen. The exact nature of the crack initiation micro–mechanism and numerical models for fatigue crack initiation are rarely discussed. The aim of this paper is precisely to elucidate the crack initiation micro–mechanism and to propose a fatigue crack initiation criterion for multiaxial loading.

3 Experimental and numerical procedures

3.1 Material

The elastomer used in the present study was a vulcanised natural rubber material (NR) filled with 23 parts of reinforcing carbon black (N772,N330) per hundred part of rubber. Formulation and mechanical properties are given on tables 1 and 2. It has to be remembered that NR does crystallized when strained at streches about 200%. Thin strip of material were cut from 150*150*2 mm rubber sheets. Those

(see numerical procedure section). In this case, due to stress softening effects, the material was first stabilised during 100 cycles at the maximal load.

TABLE 1
CHEMICAL COMPOSITION OF THE NR VULCANIZATE

Rubber	ZnO	Carbon black	Vulcanization agent
100	20.0	23.0	3

TABLE 2
ROOM TEMPERATURE MECHANICAL PROPERTIES OF THE NR STUDIED

Density (g/m^3)	A shore hardness	UTS (MPa)	$\epsilon_{failure}$ (%)	300% elongation modulus (MPa)
1.1	48	25.3	500	7.8

3.2 Fatigue testing

Fatigue testing were carried out on three types of specimens, molded by injection. The first one is a "diabolo" shaped specimen, almost uniaxial when carrying out push-pull testing. The last two are axisymmetrical notched specimens with 1.75 mm (AN2) and 4.75 (AN5) mm radius.The elastomer was bonded to the metal end pieces during the vulcanization process.
Fatigue testing were carried out under displacement control using electro–mechanical machines developed at the laboratory. Machine compliance was supposed to be largely greater than the specimen ones. Hence, the applied displacement was considered as being fully applied to the specimen and no special clip-gages was necessary.
In the case of torsion tests, the load cell was fixed to the specimen on one end and to a rigid body on the opposite end. The rigid body was able to move transversally along the specimen axis direction. Thus, pure torsion deformation was applied to the specimens and no compressive stresses induced.
Fatigue machines were supplied with waveforms generated by a digital–to–analogue converter under PC control. Cycles, force and displacement data were recorded by the PC via an analogue–to–digital converter. All tests were carried out at room temperature and at low frequency (1.5 Hz). Fatigue tests were conducted at least to crack initiation, and in most cases to rupture. The number of cycles to crack initiation (N_i) is conventionally defined as the number of cycles necessary to obtain a crack of 1mm size. N_i is difficult to determine unambiguously since neither compliance changes nor potential drop technique can be use with those materials. Hence, N_i is obtained by measurement using an optical microscope.
In the present work , the uniaxial data base was obtain from push-pull fatigue tests on diabolo specimens with strain cycles passing through zero or not. Multiaxial tests were carried out on both diabolo and axisymmetrical notched (AN) specimens by applying cyclic torsion deformation with strain cycles passing through zero or not. Moreover push-pull fatigue tests were performed on AN specimens. Push-pull tests with a superimposed static torsion angle have been found to be of prime interest to evaluate the criterion capacity to predict the crack initiation location. Experimental results obtained in a previous study [3] were added to our experimental data base.

Dissipation being lower than 3% on the stabilised strees strain curve, the material behaviour will be considered as hyperelastic non–linear, assuming homogeneity, isotropy and incompressibility. The Mooney-Rivlin model has been chosen to describe this behaviour. Rivlin showed that the strain energy function (W) may be expressed as the power series :

$$W = \sum_{i+j=1}^{n} C_{ij}(I_1 - 3)^i (I_2 - 3)^j \tag{1}$$

where C_{ij} are material parameters and I_1 and I_2 are the strain invariants of the right Cauchy–Green deformation tensor. In the present study a third order deformation expansion of the elastic potential was chosen.

$$W(I_1, I_2) = C_{01}(I_1 - 3) + C_{01}(I_2 - 3) + C_{11}(I_1 - 3)(I_2 - 3) + C_{20}(I_1 - 3)^2 + C_{30}(I_1 - 3)^3 \tag{2}$$

In this paper only stresses in the actual configuration (i.e. Cauchy stresses) will be taken into account. Cauchy stresses $\underset{\sim}{\sigma}$ are given by taking the first derivative of the strain energy function W with respect to the left Cauchy–Green tensor $\underset{\sim}{\mathbf{B}} = \underset{\sim}{\mathbf{F}}\underset{\sim}{\mathbf{F}}^T$ ($\underset{\sim}{\mathbf{F}}$ gradient tensor) :

$$\underset{\sim}{\sigma} = 2\underset{\sim}{\mathbf{B}}\frac{\partial W}{\partial \underset{\sim}{\mathbf{B}}} \tag{3}$$

C_{ij} were identified on simple extension tests results but also on finite element calculations of diabolo specimens in tension and compression. An inverse method was used and the optimisation loop was driven by the optimisation code SiDoLo, whereas finite element calculations were performed by the finite element code ZeBuLon developed at the laboratory. The term of stress imply Cauchy stress and is noted σ. 2D and 3D simulations were performed depending on the fatigue test considered.

4 Experimental and numerical results

4.1 Crack initiation location and orientation

The fatigue crack initiation location was quite evident on fracture surfaces (see figure 1).

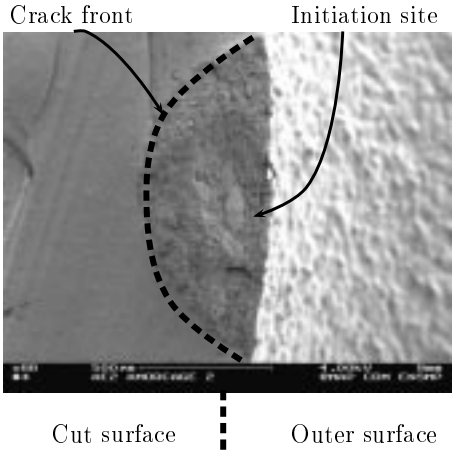

Figure 1: SEM image of a crack initiation on a cut opened AN2 specimen

In the case of push pull and torsion tests, most of the cracks initiate on or beneath the lateral surface of specimens. A very good agreement has been found between principal stress concentration zones and crack initiation locations.

Crack initiation location under push-pull with superimposed static torsion loadings are more unusual. Cracks were found to initiate inside the specimen and not at their surface where the stress concentration zone is located. Further mechanical considerations of the later case are deferred to the numerical results section.

Depending on the material, fatigue cracks can be found to appear in the direction of maximum shear amplitude (shear cracking) or maximum normal stress (tensile cracking). In our cases, the cracks initiate in such a direction that they propagate in mode I, normaly to the local maximal principal stress as shown figure 2.

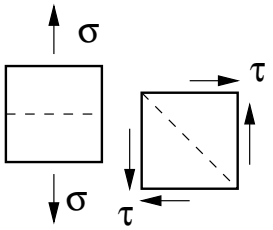

Figure 2: Cracks orientations under tension (a) and torsion (b)

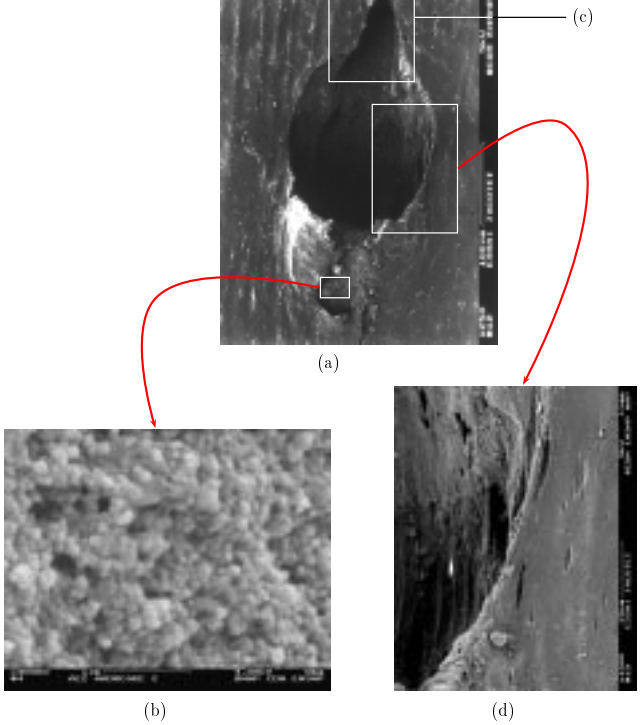

Figure 3: SEM image of a crack initiation on a diabolo specimen

4.2 Crack initiation mechanism

Figure 3–a present a Scanning Electron Microscope (SEM) image of a crack, at initiation, at the surface of a diabolo which has been push-pull tested. This picture illustrate the way by which a crack initiate.

Three zones can be distinguished :

- Figure 3–b : Energy Dispersive Spectrometry (E.D.S) reveals the presence of C, O, but not of Zn as it is the case for the rest of the specimen. A focussed view of this zone lets suppose that it is a carbon black agglomerate. The occurrence of such particles near the lateral surface can also be observed on microtomed surfaces. It has to be noticed that such particles can be found in the whole specimen and not only beneath the lateral surface. In addition, SiO_2 particles have been found at crack initiation. *Cracks initiate on rigid particles.*

- Figure 3–c : The third zone is quite similar to what can be found in the case of particle dewettering. In the case of SiO2 particles, traces of elastomer were found on the particle surface. This suggest that rupture in the binder occurs , in other words cavitation, before dewettering. OBERT and BRUENER [4], GENT and PARK [5] observed the same phenomenon on translucent rubber filled with rigid particles. They concluded that dewettering was always preceeded by cavitation. In order to observe cavitation, thin strips of rubber were pulled in tension in situ the SEM and their surface observed. Cavitation has been observed at the poles of small particles . The material being not translucent, it has not been possible to observed cavitation on larger particles (the poles are too far away from the observed surface). Nevertheless, cavitation being not size dependent (it depends only on the local stress field) [6] [7], we can suppose that the same phenomenon occurs on SiO_2 particles or CB agglomerates. Hence, *Cavitation and dewettering are the first two mechanisms in fatigue damage.*

- Figure 3–d : Fibrillation clearly appears and prove that crack propagation occurs. Initiation is considered to be obtained when this crack reaches a 1 mm size. This indicates the fact that we are dealing with the first step of a crack propagation process. we can conclude that *after cavitation and dewettering, a crack initiate and propagate up to the specimen failure.*

5.1 Loading ratio reinforcing effect

As said previously, fatigue crack propagation behaviour of crystallizing elastomers is enhance by positive loading ratios. Such reinforcing effects have been reported by many authors [1] [8] [9] and is mainly due the percistency of a crystallized zone at the crack tip during the cycle. Same results are obtained on N_i evolution. For negative loading ratios R fatigue life decreases as the stress range increases, whereas the tendancy is reversed as soon as R becomes positive.

5.2 Uniaxial criterion

5.2.1 Formulation of the criterion

Uniaxial fatigue tests results show that compressive stresses have no effect on fatigue life, in the range of compressive stresses explored [0;-4 MPa]. By closing fatigue cracks, compressive stresses do not contribute to an increase in the fatigue damage.Nevertheless, it is not possible to extrapolate these results to higher tensile compressive stresses. Indeed, Cadwell [12] has shown that large compressive stresses could damage the material, maybe by involving other physical phenomena (for instance friction under large compressive loadings) than those involved in our case. Moreover, shear stresses seem to have no effect on fatigue life since NR exibits tensile crack growth. The proposed criterion is a critical plan approach that take into account the maximal and the minimal normal stress to a plane. The critical plane is defined as the plane that experiences the maximal normal tensile stress. The minimal stress is introduced to describe the reinforcing effect. We suggest that reinforcing effect is proportionnal to the minimal crystallisation level during a cycle. The crystallisation level can be expressed as follow:

$$X_c = 0.3(1 - exp(-D. < \sigma >)) \tag{4}$$

In equation 4, σ is the normal Cauchy stress and <> denotes the MacCauley bracket (i.e. $< x >= 0.5(x + |x|)$). Using this equation, we assume that the NR crystallize at any positive tensile stress. Magnification of the macroscopic stress at the fatigue cracks tips, let us think that this assumption is reasonnable. The 0.3 coefficient refers to the 30% maximal crystallization rate for the NR under strech at room temperature [10].The number of In equation 4, σ is the normal Cauchy stress and <> denotes the MacCauley bracket (i.e. $< x >= 0.5(x + |x|)$). Using this equation, we assume that the NR crystallize at any positive tensile stress. Magnification of the macroscopic stress at the fatigue cracks tips, let us think that this assumption is reasonnable. The 0.3 coefficient refers to the 30% maximal crystallization rate for the NR under strech at room temperature [10].The number of cycles to crack initiation was correlated to the stress state via a power law function of an equivalent stress. The criterion takes the following mathematical form,

$$\sigma_{eq} = \frac{\sigma_{n\ max}}{1 + A.X_c} \text{ and } N_i = \left(\frac{\sigma_{eq}}{\sigma_0}\right)^{\alpha} \tag{5}$$

In equation 5, $\sigma_{n\ max}$ is the critical plane maximal normal stress during a cycle. A,α and D (eq. 4) are material constants, σ_0 is a normative stress and N_i is the number of cycles to crack initiation.

5.2.2 Identification of the material parameters.

There are four material constant in the current model. All four have been identify on push–pull and reverse tension fatigue tests. Stresses were obtain from FE calculations and stress values were taken at the critical point of the structure. The optimisation loop was driven by the optimisation package of ZeBuLon, using an evolutionary algorithm [11]. The optimised set of parameter is the following one :

D	A	σ_0	α
1.56	13.9	1.93	-2.7

As shown in figure 6, the model is able to correlate the fatigue lifetime within a factor of 2 scatter bands.

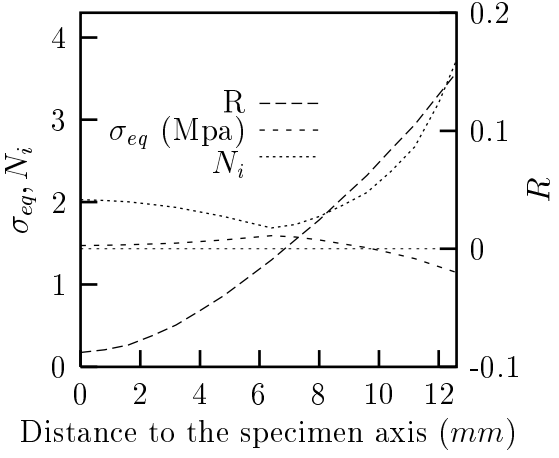

Figure 5: Evolution of several mechanical parameters along the specimen radius

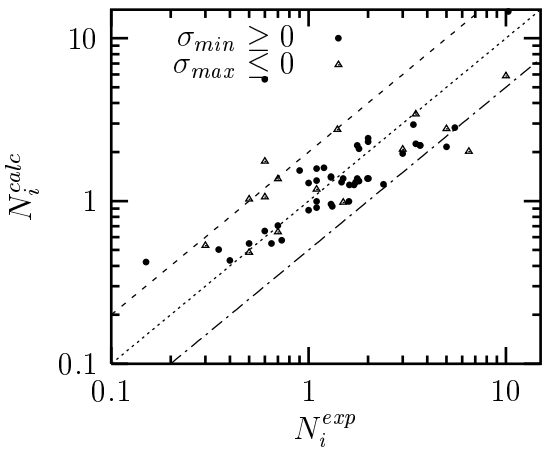

Figure 6: Push–pull results on diabolos

5.3 Multiaxial results

5.3.1 Crack initiation location

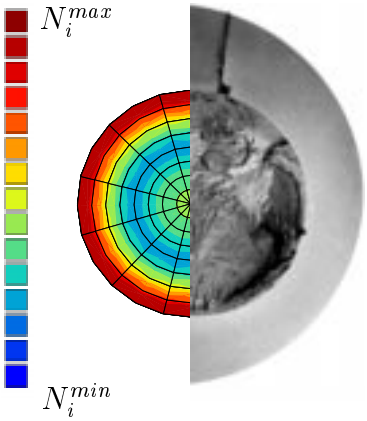

Figure 4: Comparison between crack initiation location predicted by the model and the corresponding experimental result

The criterion has been found to locate the crack initiation in all conditions of loading applied to notched and diabolo specimens, even in the case of push-pull with a superimposed static torsion as shown on figure 4. The later case can be explained if we consider the values taken by the loading ratio R at each node along the diabolo's section. Even though R is lower than zero inside the diabolo, it becomes positive at a given distance δ from the specimen axis. δ depends on the compressive load applied and decreases with increasing the algeraic value of the compressive load. Figure 5 show the evolution of the loading ratio, the equivalent stress and N_i in the cross section along the specimen radius.

5.3.2 Crack initiation prediction

Figure 7 summarizes the comparison of experimental observation and predicted fatigue life. Good results are obtained on Diabolo and AN5 specimens. Predicted lifes are within the factor of two scatter lines. Fatigue life predictions on AN2 specimens are systematically underestimated. A first attempt to explain those results was to involve a gradient effect. Indeed, AN2 specimens show a larger stress gradient than AN5 specimens. Such gradient effects have already been reported for instance by Munday and Mitchell [13] for metallic materials. However, averaging stresses, even over a large distance compared to the gradient influence distance did not lead to better results. Rather than a gradient effect, the underestimated results on AN2 specimens could be due to scale effect. The point is that two conditions have to be verified to initiate a crack. First the equivalent stress has to be sufficient, secondly a particle has to be found (remember the crack initiation mechanism). If the highly stressed zone volume is too small, no particle will be found and the crack initiation will occur somewhere else, for a lower equivalent stress i.e. a larger N_i. A probabilistic approach will be developed to take this scale effect into account.

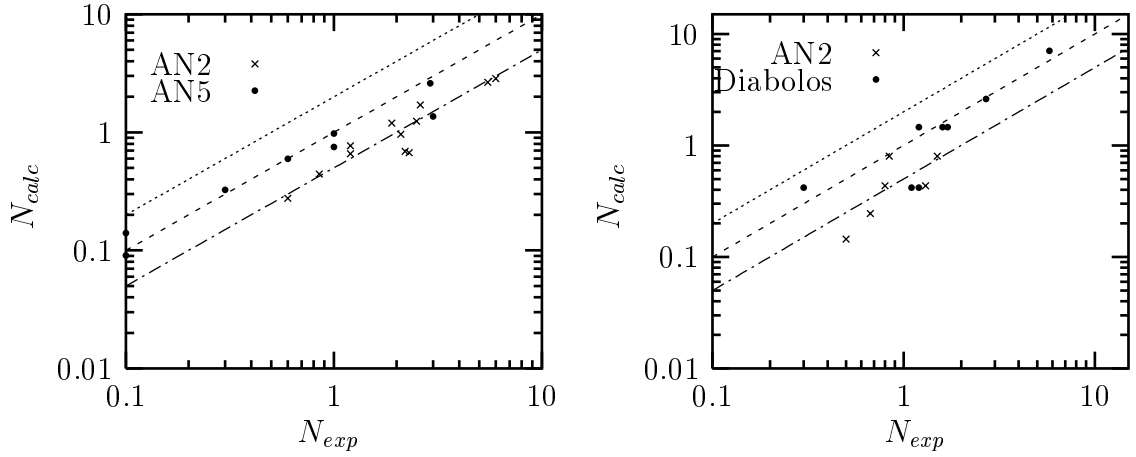

(a) Push–pull

(b) Torsion

Figure 7: Comparison between experimental and predicted N_i

6 Conclusion

From SEM observations, a fatigue crack initiation mechanism was proposed for a natural rubber vulcanizate subjected to uniaxial and multiaxial loading. Voids were found to nucleate around SiO_2 particles or Carbon black agglomerates. Cavitation and dewettering have been observed as the two mechanisms involved in the void nucleation. Then, cracks initiate from those voids and growth slowly up to the final failure of the specimen. In most cases, cracks initiate normally to the local maximum principal stress and propagate in mode I.

A fatigue crack initiation criterion has been developed. Based on a critical plane approach, it has been found to locate precisely the crack initiation and to give a good evaluation (within a factor of two) of N_i under uniaxial and multiaxial loading. In the range of stress studied, large compressive stresses have no effect on the fatigue lifetime and non-relaxing conditions increase very markedly fatigue resistance. Good results are obtained with push–pull with superimposed static torsion. As predicted by the model, cracks initiate inside the specimen and it is possible to correlate this location to the R gradient in the specimen section. Finally, a scale effect on AN2 specimen has been observed and probabilistic investigations are in progress.

7 Acknowledgements

The financial support of PAULSTRA-HUTCHINSON is greatfully acknowledged.

[1] Lindley, P.B. (1973), *Int. J. Frac.*, **9**, 449.

[2] Andrews, E. H. (1961) *J. Ap. phys.*, **23**, 542.

[3] Andre, N. (1997). PhD Thesis. E.N.S.M.P. France.

[4] Oberth, A.E. and Bruener, R.S. (1965) *Trans. Soc. Rheology*, **9**, 165.

[5] Gent, A.N. and Byougkyeu, P.,(1984) *J. of mat. sc.*, 1947.

[6] Chou-wang, M.S. and Horgan, C.O. (1989) *Int. J. Solid Structures*, **25**, 1947.

[7] Ball, J.M. (1982), *Phil. Trans. R. Soc. Lond.*, **A306**, 557.

[8] Lake, G.J. (1995) *Rubb. Chem. and Technol.*, **68**, 435.

[9] Lake, G.J. (1984) *Polymer*, **25**, 1562.

[10] Mitchell, G.R. (1971) *Rubb. Chem. and Technol.*, **45**, 309.

[11] Goldberg, D.E. (1988) *Genetic algorithms in search, optimisation, and machine learning* The University of Alabama, (Eds) Addison-Wesley.

[12] Cadwell, S.M., Merril, R.A., Slomani C.M., and Yost F.L. (1940) *Ind. and Eng. Chem.*, **12**, 19.

[13] Munday, E.G. and Mitchell, L.D. (1989) *Experimental mechanics*, 12.